Journal of Chromatography, 125 (1976) 455–469
© Elsevier Scientific Publishing Company, Amsterdam — Printed in The Netherlands

CHROM. 9157

CELLULOSE IN BEAD FORM

PROPERTIES RELATED TO CHROMATOGRAPHIC USES

J. PEŠKA, J. ŠTAMBERG, J. HRADIL and M. ILAVSKÝ

Institute of Macromolecular Chemistry, Czechoslovak Academy of Sciences, 162 06 Prague 6 (Czechoslovakia)

(First received December 2nd, 1975; revised manuscript received February 25th, 1976)

SUMMARY

Cellulose in the form of regular beads was characterized by its swelling, porosity, deformability of the individual particles expressed as the penetration modulus, and the permeability of layers in chromatographic columns. The bead cellulose possesses sufficient mechanical strength while having a considerable porosity; the flow resistance is in good accord with the spherical shape of the particles, and the allowed flow stress lies within technically useful limits. Bead cellulose has been tested as a packing in gel chromatography, and it is expected that it can be used advantageously in other chromatographic methods also, not only in its basic unsubstituted state, but also in the form of derivatives.

INTRODUCTION

Most chromatographic sorbents and phase carriers are used in the form of regular beads of a particular size. Cellulose and its derivatives are exceptions to this generalization, as up to now they have been commercially available only in the fibrous or so-called microgranular form. Although several procedures for the preparation of bead cellulose have been described[1–3], they have been used only exceptionally as chromatographic materials[4].

In this paper, a cellulose in the form of regular beads of different structure is described, which was prepared by a new procedure[5]. Properties that may affect its uses in chromatography, particularly the content of solvents in the swollen state, deformation characteristics and the column behaviour, are dealt with in detail. The applicability of the new material in gel chromatography has been demonstrated on several examples.

EXPERIMENTAL

Material

Bead cellulose was prepared according to a new procedure[5] similar to that of

Determann and Wieland[2] in that it involves the solidification of the oil suspension of a cellulose solution. The main difference is that the solidification occurs at first by heat treatment and not by the action of chemicals. The preparation of bead cellulose as well as some further chemical and physical properties are dealt with in two other papers[6,7]. Various degrees of porosity of the product were obtained by various treatments of the suspension during solidification and by various treatments of the solidified product. Samples with volume fractions of pores ranging from $P = 0$ to 0.8 can be prepared by this procedure. Samples exhibiting the highest porosity were not completely stable during drying and were therefore stored in the swollen state with sodium azide added as a bacteriostat. Samples with low porosity can be dried without change.

Bead cellulose was thoroughly washed with water prior to measurements. Fractions of particular sizes were obtained by sieving in water. The separate samples were characterized by the bed volume of the swollen material relative to its weight in the dry state (ml/g). Microphotographs of the bead and fibrillar and microgranular cellulose were obtained with an Exacta apparatus with an extension for close photographing. The samples were dry and lit from above.

Swelling and porosity

Swelling was determined with centrifugal columns described elsewhere[8]. The samples were swollen to equilibrium in water or methanol, centrifuged (1400 *g*) and weighed. The procedure was repeated several times until constant values were obtained. On drying *in vacuo* at room temperature, the measurement was repeated and the sample was dried again. The results obtained were used to calculate the weight swelling in grams of the solvent per gram of the dry matter; for methanol, the weight swelling was re-calculated by dividing by the methanol density, which yielded a comparable quantity, the volume swelling in millilitres of the solvent per gram of the dry matter. In both instances the porosity was also calculated, *i.e.*, the volume fraction of the solvent in the swollen sample. The volume of the substance was calculated from the specific gravity (1.52) for the basic regenerated cellulose.

Deformation characteristics

A theoretical solution of the problem of stress distribution between two spherical bodies in contact with each other was first postulated by Hertz for the case of the validity of Hook's law between stress and strain. Assuming contact between two beads that have radii r_1 and r_2, the theory[9] predicts that the total pressure force, F, is given by

$$F = \frac{16}{3(x_1 + x_2)} \cdot \left(\frac{r_1 r_2}{r_1 + r_2}\right)^{1/2} \cdot d^{3/2} \qquad (1)$$

where d is compression, *i.e.*, a change in the distances between parts of the beads undeformed by pressure, and $x_i = 4(1 - \mu_i^2)/E_i$ $(i = 1, 2)$, where μ_i and E_i are Poisson's constant and Young's modulus of the material, respectively.

From eqn. 1, in the application to our particular procedure, the deformation of the bead between two planes having a high Young's modulus ($r_1 = r$, $E_1 = E$, $x_1 = x$, $r_2 \to \infty$, $E_2 \to \infty$, $x_2 = 0$) gives

$$F = (16/3)\, A\, r^{1/2} (\Delta y/2)^{3/2} \qquad (2)$$

where $A = 1/x$ is the penetration modulus and $\Delta y = y_0 - y$ is a change in the distances of the deformation planes in the undeformed and deformed states. If the material is incompressible ($\mu = 1/2$), $A = G = E/3$, where G is the shear modulus. Eqn. 2 is similar to the relationship derived for the penetration of a bead with a diameter r and a high penetration modulus into an elastic plane[10,11], which is a consequence of the symmetry of eqn. 1 with respect to subscripts 1 and 2.

Deformation measurements on the individual beads compressed between two plates were carried out on a simple apparatus (Fig. 1). The force value was measured with an inductive force transducer connected with a bridge (KWS-2, Hottinger Baldwin Messtechnik, G.F.R.) and recorded with a recorder (accuracy $\pm$ 1 mN). The deformation was imposed by means of a screw and conveyed with a rod firmly connected with the force transducer; its value was read off using a deformation indicator with an accuracy of $\pm$ 0.001 mm. In the determination of the deformation value, a correction was made for the deformation of the membrane of the force transducer with increasing load. The surfaces in contact with the sample were made of PTFE in order to provide the best possible sliding of the sample surface on the bearing plate. Special care was taken to obtain the highest possible parallelism of the two PTFE surfaces. During measurements, the samples were surrounded by the solvent in which they were swollen to equilibrium; the measurement was carried out at constant temperature (20°).

Prior to the deformation measurement, the diameter of the bead was determined by means of an Abbé comparator with an accuracy of $\pm$ 0.002 mm, each time for at least three different positions of the bead. The mean of the three values was used in further calculations. The individual diameters were found to differ by only

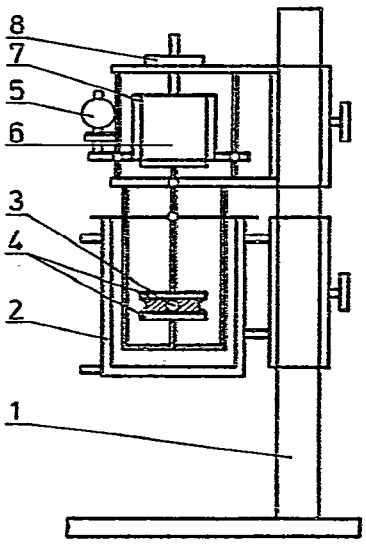

Fig. 1. Apparatus for measurement of mechanical characteristics. 1 = Holder; 2 = thermostating cylinder; 3 = sample; 4 = PTFE plates; 5 = deformation indicator; 6 = force transducer, 7 = thermostating cylinder for 6; 8 = micrometer screw.

1–2%, which suggests a good spherical shape of the samples. The bead was then transferred into a deformation apparatus and compressed to the lowest deformation y_1 and the change in the force F with time was recorded. After a chosen constant time of 2 min, the force F_1 corresponding to the compression y_1 was read off. The deformation was then increased and the whole process repeated. At least 20 values of y_i and F_i were measured on each sample, and at least two beads were taken for each system. However, the values of F_i cannot be regarded as the equilibrium values, because for samples with a low modulus in particular, a pronounced time dependence of F was observed, indicating a considerably viscoelastic character of deformation of such samples. Because of the purpose of this work, this time dependence was not studied in more detail.

For the direct treatment of the experimental data, eqn. 2 was applied in the form

$$F_i^{2/3} = \frac{1}{2}\left(\frac{16}{3} A r^{1/2}\right)^{2/3} (y_0 - y_i) = C - S y_i \tag{3}$$

where C and S are constants. The advantage of such a plot consists in its invariance with a shift of the origin at y_i : y_0 need not be known for determining A. Also, the absolute values of y_i are not important, so that the y_i values directly read off from the scale of the deformation indicator can be used. A was determined from the slope S according to the equation

$$A = 3(2S)^{3/2}/16r^{1/2} \tag{4}$$

The assumption used for deriving eqn. 2 about the high modulus of surfaces of the deformational apparatus was checked by direct measurement. The same time procedure as described above was used for the investigation of the penetration of a steel bead into a PTFE plate[10,11]. The penetration modulus for PTFE calculated from eqn. 2 was 190 MPa, that is, higher by one or two orders of magnitude than the moduli determined for the samples investigated.

Flow-rate

The hydrodynamic resistance of the layer in the column was measured in a flow of de-gassed distilled water. A sorbent column, 9 mm in diameter and 30–60 mm high, was supported by a network of stainless steel with holes of diameter 0.01 mm. The pressure above the column was measured with a metallic manometer of the Bourdon type; the flow-rate was calculated from direct measurements of time and the amount of water that had left the column. For higher flow-rates, the instantaneous flow-rate was read off from a rotameter placed behind the column. The readings were calibrated by direct measurements. The hydrodynamic resistance of an empty apparatus was also determined; it was found that the pressure losses in the empty apparatus at the flow-rates under investigation were negligible, so that no correction was needed.

Gel chromatography

A K-2 chromatograph provided with a refractive index detector (Waters R403) was manufactured in the workshops of the Institute of Macromolecular

Chemistry of the Czechoslovak Academy of Sciences. Stainless-steel columns (120 cm × 0.81 cm I.D.) were filled with an aqueous suspension of the sorbent at a pressure of 0.5–1 MPa. The test compounds were injected in doses of 2 ml of 1% aqueous solution. De-gassed distilled water was used as the eluent. The distribution coefficients, effectivities and the useful range of molecular masses were calculated from the results according to the literature[12].

RESULTS AND DISCUSSION

In Fig. 2, bead cellulose is compared with typical samples of commercial chromatographic cellulose. It can be seen that the shape of the particles resembles those of other chromatographic materials, ion exchangers and copolymers for gel and affinity chromatography.

The content of solvents in the swollen bead cellulose and the degrees of swelling and porosities derived therefrom were calculated from a number of measurements, illustrated by an example in Fig. 3. Fig. 3 shows that the weight of the dry sample is reproducible, which suggests that no extraction of soluble fractions occurred during washing. The results are summarized in Table I. It was found that the samples of bead cellulose dealt with in this work reached the same porosities as those of the dextran gels Sephadex G-25 and G-50. Consequently, they are much more porous than most of the usual macroreticular ion exchangers and chromatographic materials. Although the bead cellulose described here is a material that was not additionally chemically cross-linked, the samples can be cautiously dried. The measure of preservation of porosity after re-swelling can be seen from a comparison of the values I

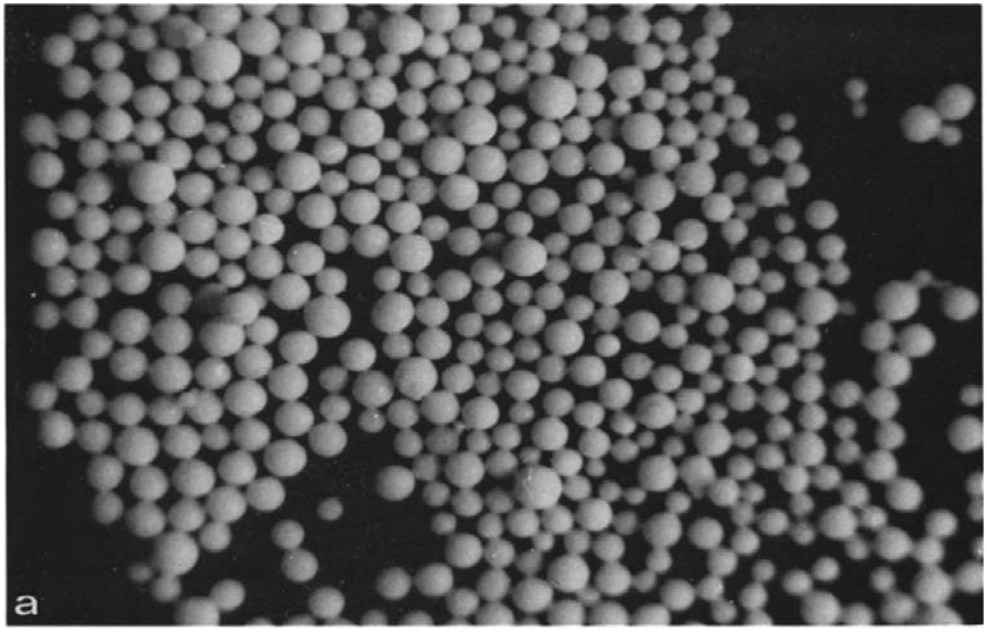

Fig. 2.

(Continued on p. 460)

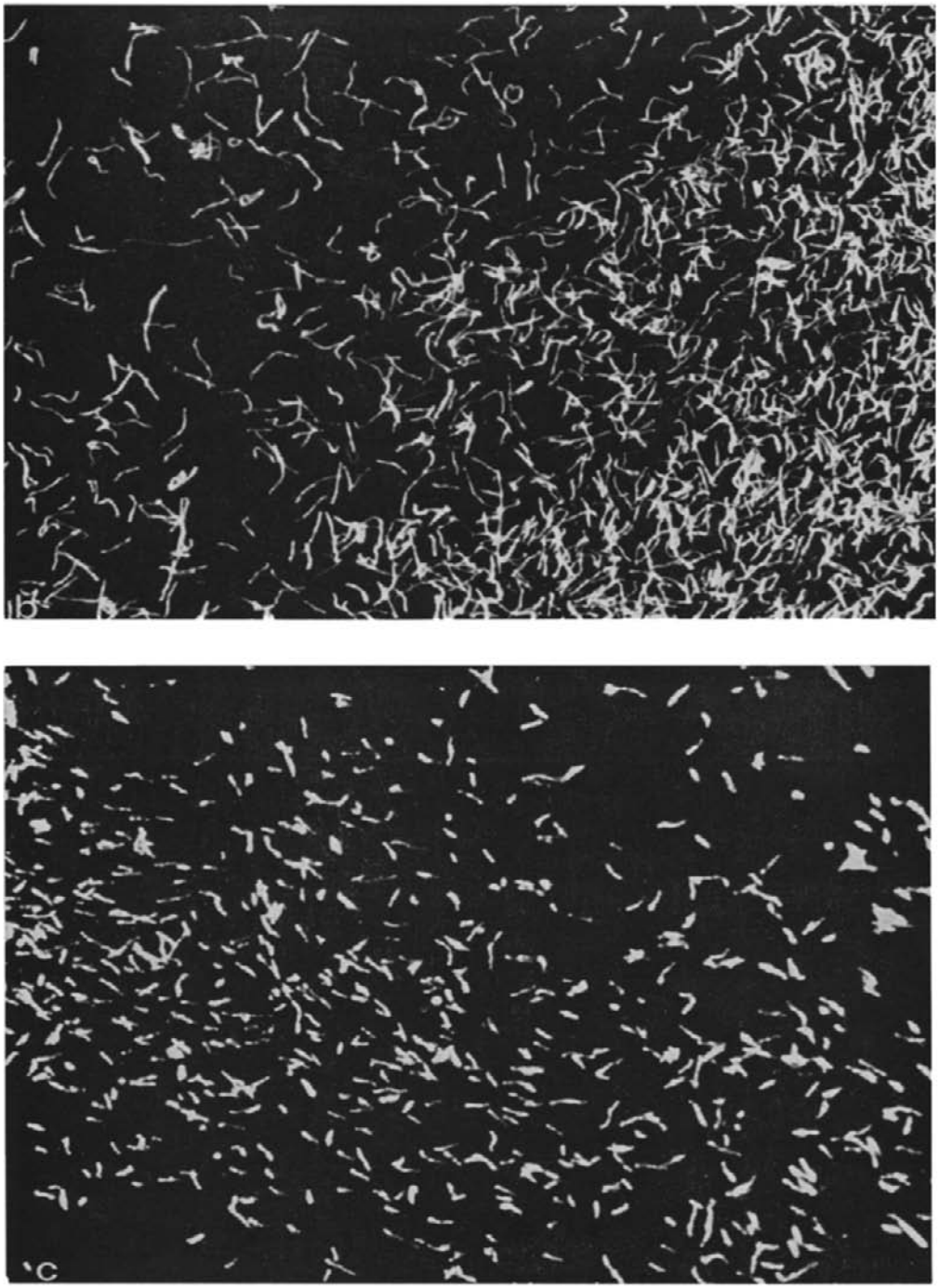

Fig. 2. Microphotographs of (a) bead cellulose No. 12, (b) standard-grade cellulose for chromatography and (c) microgranular cellulose.

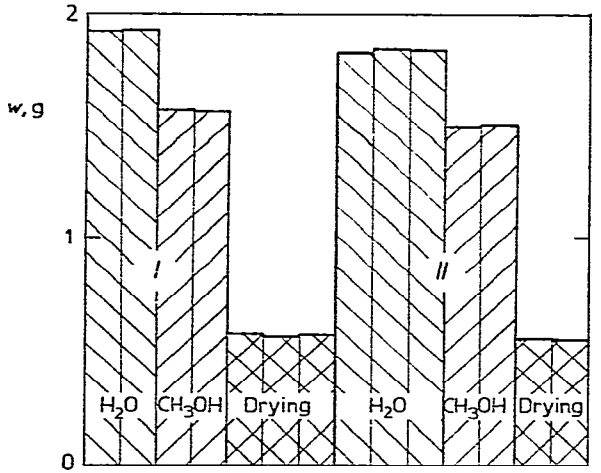

Fig. 3. Example of determination of swelling. Bead cellulose No. 1; sample weight (w) during determination of swelling.

and II (Fig. 3 and Table I). The character of the porosity can be estimated by comparing the swelling values in water and methanol (better and poorer swelling agent, respectively, for cellulose). In a limiting case of capillary porosity, one should expect the same swelling in both solvents, while the swelling porosity would be reflected by a very low swelling in methanol. The observed low decrease in porosity in methanol compared with that in water (Table I) indicates that both types of porosity are present, but that the capillary porosity predominates over the swelling porosity.

The deformation behaviour of the individual particles was characterized by the penetration modulus A defined by eqn. 2. A typical example of the reading of the modulus A is given in Fig. 4, where the dependence of $F^{2/3}$ on y is plotted, F being the

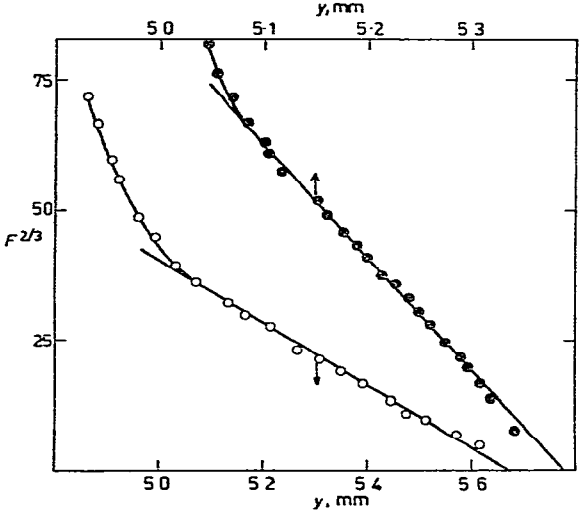

Fig. 4. Example of determination of penetration modulus. Deformation characteristic of bead cellulose No. 6 (●) and No. 10 (○) (bed volumes 4.1 and 10 ml/g, respectively). F, force (mN); Δy, deformation.

TABLE I

SWELLING OF BEAD CELLULOSE

No.	Sample		Swelling I*			Swelling II*			Porosity I		Porosity II	
	Bed volume (ml/g)	Bead size (mm)	H_2O (g)	CH_3OH (g)	CH_3OH (ml)	H_2O (g)	CH_3OH (g)	CH_3OH (ml)	H_2O (%)	CH_3OH (%)	H_2O (%)	CH_3OH (%)
1	5.0	0.25–0.16	2.34	1.71	2.15	2.28	1.66	2.10	78.1	76.6	73.6	76.2
2	7.1	0.25–0.16	3.36	2.58	3.25	2.16	1.58	1.99	83.6	83.2	76.7	75.2
3	6.9	0.25–0.16	3.48	2.55	3.22	2.19	1.53	1.93	84.1	83.0	76.9	74.6

* Swelling given is the amount of solvent per gram of dry sample; I = original sample, II = the same sample after drying to constant weight and swollen again to equilibrium.

force and Δy being the corresponding deformation. Fig. 4 shows that in the initial region of compression a linear dependence can be found, in agreement with the value predicted theoretically by eqn. 3; the penetration modulus was calculated from the slope of the linear part according to eqn. 4. The linear region is unexpectedly large and is about 40–50% of the total diameter of the bead for samples with low moduli. With increasing modulus A, its width decreases (Fig. 4). At higher compressions, one can observe a faster increase in $F_t^{2/3}$ with y_t, which means that A also increases with y_t. However, one may expect that in this region Hook's law, on which eqn. 2 is based, ceases to be valid. Another possible explanation of this deviation may consist in insufficient sliding of the bead surface on PTFE bearing plates.

In order to find the extent to which the values of the modulus A depend on the size of the sample, we measured beads of one system with radii ranging from 0.2 to 0.6 mm. Fig. 5 shows that the A values for $r > 0.4$ mm are virtually independent of the radius, while for $r < 0.4$ mm the values of the moduli increase with decreasing r. Similar results were found for the method involving the penetration of a solid bead into an elastic bearing plate[10], where the penetration modulus was found to increase with decreasing thickness of the plate and with increasing radius of the penetrating bead. In pressure tests on cylindrical samples it was also found that with a decreasing ratio of height to diameter of the cylinder the penetration modulus increases[13]. These results were explained by imperfect sliding of the sample surface on the plates. With respect to the above results, measurements on samples that have possibly identical radii, 0.5–0.7 mm, are included in Table II; these measurements are not affected by the bead size to any substantial extent (*cf.*, Fig. 5). The highest A values (for dry samples, Table II) can be subject to a *ca.* 10% error, because they are lower by only one order of magnitude than the modulus of PTFE used in the deformation apparatus.

For comparison, Table II also includes the modulus values for samples of some commercial ion exchangers. It can be seen that the swollen bead cellulose exhibits modulus values of the same order of magnitude as those for the swollen

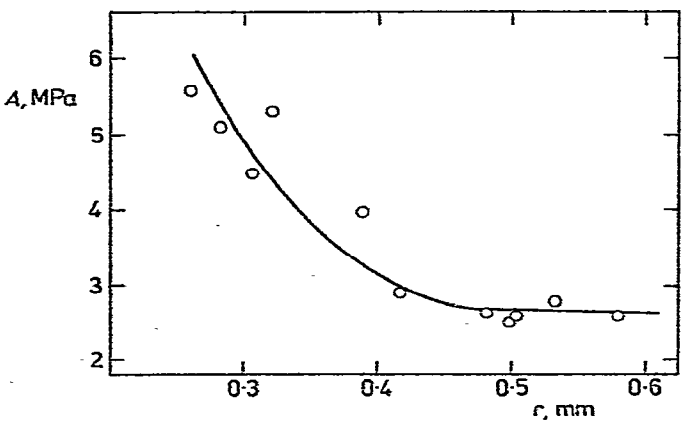

Fig. 5. Dependence of penetration modulus (A) on particle diameter (r). Bead cellulose No. 6 (bed volume 4.1 ml/g).

TABLE II

MECHANICAL CHARACTERISTICS OF BEAD MATERIALS

Swollen bead cellulose			*Dry bead cellulose*			*Swollen commercial ion exchangers*		
No.	*Radius, r (mm)*	*Penetration modulus, A (MPa)*	*No.*	*Radius, r (mm)*	*Penetration modulus, A (MPa)*	*Name*	*Radius, r (mm)*	*Penetration modulus, A (MPa)*
6*	0.533	2.80	8	0.347	24.73	Zerolit***	0.535	1.44
	0.503	2.36		0.332	25.84		0.605	1.50
	0.500	2.46	9	0.419	17.21		0.700	1.35
	0.483	2.63		0.408	20.74		0.638	1.30
7**	0.610	0.44				Zerolit§	0.692	0.28
	0.605	0.44					0.834	0.27
	0.615	0.34				Amberlite§§	0.510	27.62
	0.590	0.41					0.473	26.92
	0.595	0.59						

* Bed volume 4.1 ml/g.
** Bed volume 8.45 ml/g.
*** Carboxylic cation exchanger Zerolit 226 (H^+).
§ Zerolit 226 in equilibrium with 0.01 *N* NaOH.
§§ Strongly acid styrene sulphonic cation exchanger Amberlite IR-120 (H^+).

carboxylic cation exchanger; the values found for dry bead cellulose are comparable with those for swollen styrene ion exchangers, represented in this instance by Amberlite IR-120. For two samples of swollen cellulose, important differences in the values of the modulus A can be observed, which in Table II are related to the bed volume. The latter reflects the equilibrium swelling or porosities. As expected, a lower modulus was found for the more swollen sample.

The behaviour of sorbents in a flow of water is shown in Figs. 6 and 7 as a dependence of the linear flow rate, U (m/h) (flow-rate relative to an empty cross-section of the column), on the pressure gradient B (cm H_2O/cm). Curve 2 (Fig. 6), obtained with dextran gel, is typical of materials subjected to deformation. At low pressure gradients, there is a linear region characterized by the slope K_0 which is sometimes referred to as the specific permeability. At higher pressure gradients, the linear relationship ceases to hold, because the particles become deformed and the free space in the column is reduced, thus reducing the permeability of the layer. In general, the curves pass through a maximum, and in soft sorbents the flow-rate decreases to zero, which happens when the column becomes clogged owing to the destruction of particles. The slope of the linear part is determined only by the particle size and form, while the region of non-linear behaviour is determined predominantly by the deformability of the material.

In Fig. 6, bead cellulose is compared with some dextran gels. Curve 1 relates to bead cellulose, while curve 2 relates to bead dextran of comparable bead size. The full line indicates the initial slope calculated for a given particle size according to the literature[14]. It can be seen that bead cellulose and bead dextran differ markedly, especially in the non-linear part. The effect of the bead form is stressed if a comparison is made with earlier gels with an irregular shape. Their behaviour is illustrated by the individual points in the bottom part of Fig. 6. Although their particle size is

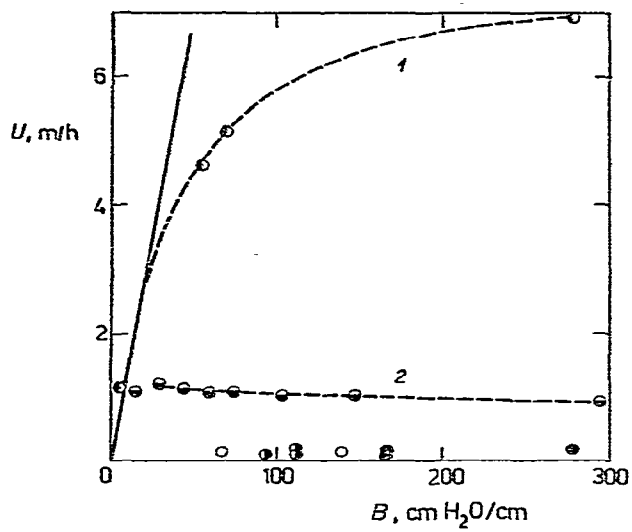

Fig. 6. Flow characteristics: comparison of bead cellulose with dextran gels. ◐, Bead cellulose No. 11 (bed volume 7.9 ml/g, bead size 20–60 μm); ◒, bead dextran gel (bed volume 10 ml/g, bead size 20–100 μm) (Sephadex G 50 Superfine). Dextran gels of irregular shape: ○, bed volume 5 ml/g, bead size 40–130 μm; ●, bed volume 5 ml/g, bead size 90–240 μm; ◑, bed volume 13 ml/g, bead size 110–390 μm. *U*, Linear flow-rate; *B*, pressure gradient.

larger than that of the two other sorbents and the degrees of swelling are not too different, their permeabilities are very low. Fig. 7 illustrates the effect of the bead size of the sorbent. Curve 1 is the same as curve 1 in Fig. 6 and corresponds to a

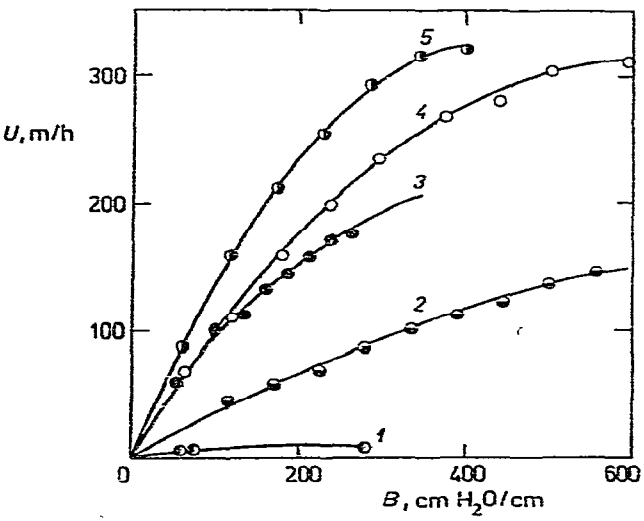

Fig. 7. Flow characteristics of bead cellulose; effect of bead size. ◑, No. 1 (bed volume 5.0 ml/g, bead size 140–250 μm); ○, No. 3 (bed volume 6.9 ml/g, bead size 140–250 μm); ●, No. 2 (bed volume 7.1 ml/g, bead size 140–250 μm); ◒, No. 2 but after being subjected to a gradient of 1000 cm H_2O/cm for 2 h; ◐, No. 11 (bed volume 7.9 ml/g, bead size 20–60 μm) (the same data as the upper curve in Fig. 6 on a different scale). *U*, linear flow-rate; *B*, pressure gradient.

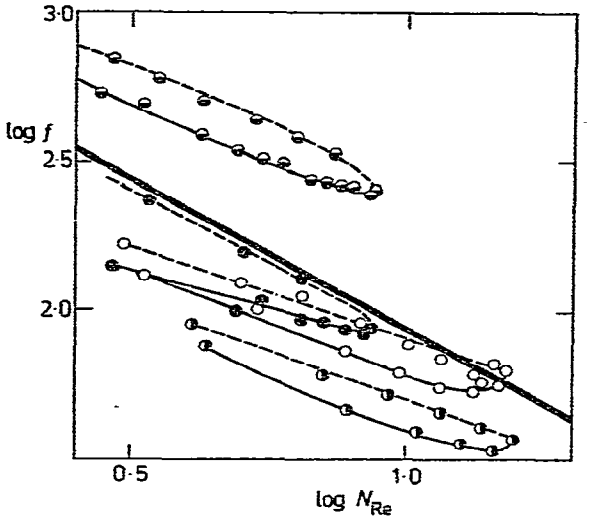

Fig. 8. Flow characteristics of bead cellulose in Fannig's correlation. Log–log plot of frictional coefficient (f) as a function of Reynolds number (N_{Re}). Behaviour after release of tension (reverse dependences) denoted by broken lines. ◑, No. 1 (bed volume 5.0 ml/g, bead size 140–250 μm); ○, No. 3 (bed volume 6.9 ml/g, bead size 140–250 μm), ◉, No. 2 (bed volume 7.1 ml/g, bead size 140–250 μm); ◒, No. 2, but after being subjected to a gradient of 1000 cm H_2O/cm for 2 h.

finely granulated bead cellulose. Curves 3–5 are related to samples of bead cellulose with coarser particles. Of these, the softest sample was selected and loaded with a pressure gradient of 1000 cm H_2O/cm for several hours. A comparison of curve 3 (before load) and curve 2 (after load) indicates some decrease in permeability. With soft dextran gels, the column is completely clogged under such conditions.

The deformation of particles and the departure from linear behaviour due to it are represented better by Fanning's correlation[14]. In Fig. 8, the logarithm of the non-dimensional frictional coefficient, f, is plotted against the logarithm of the modified Reynolds number, N_{Re}, where

$$f = D\,\Delta p/2\,L\varrho U^2\alpha$$
$$N_{Re} = DU\varrho/\mu \qquad (5)$$

where ϱ and μ are the specific mass and viscosity of the flowing liquid, respectively, U is the linear flow-rate, Δp is the pressure drop, L is the layer height, D is the nominal diameter of the particles and α is the wall factor. For non-deforming spheres of uniform size, the empirical relationship

$$\log f = 2.93 - \log N_{Re} \qquad (6)$$

holds over the whole range of laminar flow[14]. This dependence is represented in Fig. 8 by the heavy line. In this correlation, deformation and a decrease in the flow-rate are reflected in an increase in $\log f$ and in an increase in slope in eqn. 6 above the

theoretical value of −1 up to positive values. Fig. 8 also involves the reverse curves, obtained by decreasing the pressure gradient (broken lines). In general, there are two limiting cases. Lasting deformation causes the linear reverse shoulder to shift towards higher log f values, while the theoretical slope −1 remains unchanged. Elastic deformation results in a return to the original values. Fig. 8 shows that the samples of bead cellulose described here possess both deformational components, and that the viscoelastic component is greatly dependent on time.

Thus, the flow properties give evidence about the deformability of particles in a similar manner to the penetration modulus. However, no direct comparison is feasible, because the flow properties were measured on samples other than that for the modulus; the samples used for the determination of the modulus had to be coarse and therefore required separate preparation. The connecting quantity for both determinations is the bed volume. As expected, samples with a small bed volume have the highest penetration modulus (Table II) and are those least deformed at pressure loads in the column (Figs. 7 and 8).

The gel chromatographic properties of bead cellulose were investigated on two types of samples, with different bed volumes. Data characterizing the samples and the separation effectivity are summarized in Table III. The resolving power of the gel is expressed in terms of the coefficient $\beta = \Delta K_{av}/\Delta \log M_W$, which describes the gel property independent of the geometry of the columns. The type A samples (Nos. 4 and 13), having higher porosity, appear to be a universal gel for a wide range of molecular weights; on the other hand, this is accompanied by a lower resolving power. The resolving power of the type B samples (Nos. 5 and 12) is higher; the separation occurs within a narrower range of molecular weights. Table III also shows that the heights equivalent to a theoretical plate depend mainly on the bead size. This could be further reduced only by introducing finer particle separation techniques than separation of the adsorbent on wet sieves. The measurements were reproducible during 1 month. As follows from the elution volumes of strongly polar compounds (Table IV), bead cellulose did not exhibit non-specific sorption that would be reflected in an increase in the elution volumes above the expected value, or

TABLE III

GEL CHROMATOGRAPHIC PROPERTIES OF BEAD CELLULOSE

Sample			*Exclusion limits*		*Outer volume, V_0 (ml)*	*Total volume, V_0+V_i (ml)*	*Coefficient of resolving power, β**	*Column efficiency**, HETP (cm)*	
No.	*Bed volume (ml/g)*	*Bead size (mm)*	*Upper, M_{W_0}*	*Lower, M_{W_1}*				*D-2000*	*CH_3OH*
4	10	0.31–0.12	$5\cdot10^5$	300	26.63	38.06	0.13	7.5	6.5
5***	5.8	0.15–0.07	$2\cdot10^5$	$2.5\cdot10^3$	20.93	41.87	0.27	2.2	2.2
5§	5.8	0.15–0.07	$2\cdot10^5$	$2.5\cdot10^3$	20.93	39.95	0.27	2.2	1.4
12	6	0.08–0.02	$5.6\cdot10^5$	$2\cdot10^4$	5.00	7.26	0.61	3.4	1.0
13	10	0.05–0.03	$5\cdot10^5$	500	24.24	38.29	0.124	1.7	0.5

* $\beta = \Delta K_{av}/\log M_W$.

** Calculated according to ref. 12 for dextran D-2000 or methanol.

*** First measurement.

§ Second measurement after 1 month.

TABLE IV

ELUTION VOLUMES OF POLAR COMPOUNDS ON BEAD CELLULOSE

Compound	*Sample 4*			*Sample 5*		
	Elution volume, V_e (ml)	K_{av}	*H (cm)*	*Elution volume, V_e (ml)*	K_{av}	*H (cm)*
Ethanolamine	38.06	0.329	4.8	36.15	0.376	9.2
Tetramethylammonium hydroxide	39.96	0.383	5.5	39.96	0.470	3.8
Pyridine	43.76	0.493	7.5	47.86	0.512	3.0
Acetic acid	41.86	0.438	6.8			
Glucose	41.86	0.438	5.6	41.86	0.517	3.9
Ethylene glycol	39.96	0.383	4.9	41.86	0.517	2.2
Methanol	39.96	0.383	4.1	39.96	0.470	1.7

in excessive tailing. Fig. 9 shows the dependence of the distribution coefficient, K_{av}, on the molecular weight of a number of polydextrans and low-molecular-weight compounds.

Samples of type B (bed volume *ca.* 6 ml/g, Table III) resemble the dextran gel Sephadex G-100 in their exclusion limits (bed volume 15–20 ml/g)[15]. The considerable difference in the bed volumes indicates the different character of the porosity of the two types of samples. Bead cellulose resembles macroporous materials, while the dextran gel exhibits only swelling porosity and consequently must swell three times as much to reach the same pore size. The higher swelling of the dextran gel leads to a correspondingly higher deformability and to a lower admissible pressure gradient, in accordance with what has been said earlier.

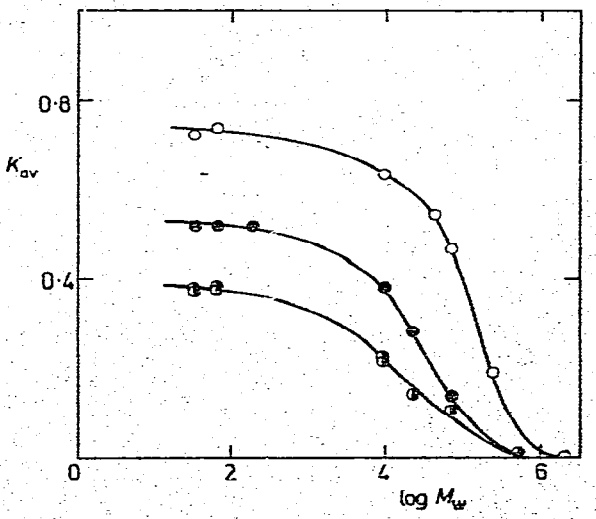

Fig. 9. Dependence of distribution coefficient (K_{av}) on log M_w of the test series of polydextrans and low-molecular-weight compounds. K_{av} calculated according to the literature[12]. ◑, Samples No. 4 and 13; ●, sample No. 5; ○, sample No. 12.

CONCLUSION

The bead cellulose described here is a new chromatographic material with various porosities, a low resistance in the column and suitable for use in gel chromatography. As reported elsewhere[6], bead cellulose can be chemically transformed into ion-exchange derivatives and other special adsorbents without damaging the spherical shape of the particles; consequently, similar advantages can be expected for its application in other chromatographic procedures, *e.g.*, in ion-exchange and partition chromatography.

REFERENCES

1 J. J. O'Neill, Jr., and E. R. Reichardt, *U.S. Pat.*, 2,543,928 (1951); *C.A.*, 45 (1951) 4927c.
2 H. Determann and T. Wieland, *Fr. Pat.*, 1,575,419 (1969); *C.A.*, 73 (1970) 16545z; *U.S. Pat.*, 3,597,350 (1971); *C.A.*, 75 (1971) 130959d; *Makromol. Chem.*, 114 (1968) 263.
3 K. Yasui, Y. Isome, K. Sugimori and S. Katsuyama, *Jap. Pat.*, 73-60,753 (1973); *C.A.*, 80 (1974) 15951m; K. Yasui and S. Katsuyama, *Jap. Pat.*, 73-21,738 (1973); *C.A.*, 79 (1973) 55153p.
4 K. Chitumbo and W. Brown, *J. Chromatogr.*, 80 (1973) 187.
5 J. Peška, J. Štamberg and Z. Blače, *Czech. Pat. Appl.*, PV 3858-74 (1974).
6 J. Peška, J. Štamberg and J. Hradil, *Angew. Makromol. Chem.*, in press.
7 J. Baldrian, J. Peška, J. Štamberg, J. Ludwig and D. Paul, *Symp. on Advances in the Chromatographic Fractionation of Macromolecules, Birmingham, 1976*, to be presented.
8 J. Štamberg and S. Ševčík, *Collect. Czech. Chem. Commun.*, 31 (1966) 1009.
9 Z. Horák, F. Krupka and V. Šindelář, *Technická Fyzika*, SNTL, Prague, 1961, p. 314.
10 N. E. Waters, *Brit. J. Appl. Phys.*, 16 (1965) 557.
11 D. J. Walsh, G. Allen and G. Ballard, *Polymer*, 15 (1974) 336.
12 H. Determann, *Gelová Chromatografie*, Academia, Prague, 1972, pp. 78, 83, 84.
13 J. Hasa, *Collect. Czech. Chem. Commun.*, 39 (1974) 1029.
14 J. H. Perry, *Chemical Engineering Handbook*, McGraw-Hill, New York, 3rd ed., 1950, p. 393.
15 *Sephadex, Gel Filtration in Theory and Practice*, Pharmacia Fine Chemicals, Uppsala, 1974.